PHYSICAL REVIEW B **73**, 085316 (2006)

# Effects of non-parabolicity and in-plane magnetic fields on the cyclotron effective mass and $g_\perp$-factor in GaAs-(Ga,Al)As quantum wells

M. de Dios-Leyva,[1] E. Reyes-Gómez,[1] C. A. Perdomo-Leiva,[2] and L. E. Oliveira[3]
[1]*Department of Theoretical Physics, University of Havana, San Lázaro y L, Vedado 10400, Havana, Cuba*
[2]*Departamento de Física, ISPJAE, Calle 127 s/n, Marianao 19390, Havana, Cuba*
[3]*Instituto de Física, Unicamp, CP 6165, Campinas, São Paulo, 13083-970, Brazil*
(Received 17 October 2005; revised manuscript received 4 January 2006; published 16 February 2006)

The envelope-function approach is used to theoretically study the effects of in-plane magnetic fields on the cyclotron effective mass and Landé $g_\perp$-factor associated to conduction electrons in single GaAs-(Ga,Al)As quantum wells. Non-parabolic and anisotropy effects are included in the calculations within the Ogg-McCombe effective Hamiltonian to describe the electron states in the semiconductor heterostructure. The electronic structure and both the cyclotron effective mass and Landé $g_\perp$-factor were obtained, by expanding the corresponding envelope wave functions in terms of harmonic-oscillator wave functions, as functions of the in-plane magnetic field, cyclotron orbit-center position, and quantum-well widths. This procedure allows us to consider the different terms in the Hamiltonian on equal footing, avoiding therefore the use of approximate methods to obtain the envelope wave functions and the corresponding energy spectrum. Results obtained for the Landé $g_\perp$-factor were found in quite good agreement with available experimental measurements.

DOI: 10.1103/PhysRevB.73.085316 PACS number(s): 71.18.+y, 71.70.Ej, 73.21.Fg, 78.20.−e

## I. INTRODUCTION

The physical properties of low-dimensional semiconductor systems have been widely studied in the past few decades. Quantum wells (QWs), quantum-well wires (QWWs), quantum dots (QDs), superlattices (SLs), and so on, have been the subject of considerable efforts in order to elucidate their physical nature. It is important to point out that the understanding of the electronic properties of semiconductor heterostructures has made possible the fabrication of a number of electronic and opto-electronic devices. The electronic structure of these semiconductor nanosystems may be modified by different factors, such as the presence of confining potentials, externally applied electric and magnetic fields, hydrostatic pressure, etc., leading to changes on their electronic and optical properties. The transport of spin-polarized electrons by using ferromagnetic probe tips in a low-temperature scanning tunnelling microscope opened up the possibility of investigating magnetic systems at spatial resolutions in the angstrom scale.[1–3] The ability to manipulate single spins[4–7] is one of the important aspects in the development of quantum information processing and spintronics. Due to the increasing potential applications in a new variety of semiconductor devices based on spin-electronic transport, the study of both cyclotron-resonance properties[8–11] as well as the behavior of the Landé $g$-factor[12–19] in nanostructured systems has attracted the community attention, and a considerable amount of work has been carried out in this area. From the experimental point of view, the Landé factor is measured by using a number of experimental techniques, such as electron spin resonance,[12,13] Hanle effect,[14] spin quantum beats,[15–18] spin-flip Raman scattering,[19] capacitance,[20] and energy,[21,22] spectroscopies. The measurement of the Landé factor in semiconductor heterostructures is of interest for several reasons. For instance, it plays a relevant role in the integral and fractional quantum Hall effects,[13,23–25] or in phenomena involving efficient optical pumping[26] of electron and nuclear spin of individual GaAs QDs. The dependence of the electron Landé factor on carrier quantum confinement in QWs and QDs has recently gained attention both experimentally[18–26] as well as theoretically.[27–30] The $g$-factor of electrons in GaAs-$Ga_{1-x}Al_xAs$ QWs is of special interest, as it changes its sign at certain values of the well width. Hannak *et al.*[16] determined the electron Landé factor as a function of the GaAs-$Ga_{1-x}Al_xAs$ well width from 1 to 20 nm under in-plane magnetic fields by the technique of spin quantum beats. Le Jeune *et al.*[17] studied the anisotropy of the electron Landé factor in GaAs QWs, whereas Malinowski and Harley[18] investigated the influence of quantum confinement and built-in strain on conduction-electron $g$ factors in $GaAs/Al_{0.35}Ga_{0.65}As$ QWs and strained-layer $In_{0.11}Ga_{0.89}As/GaAs$ QWs, for QW widths between 3 and 20 nm.

The aim of the present work is to investigate the effects of in-plane magnetic fields on the cyclotron effective mass and Landé $g_\perp$-factor in GaAs-$Ga_{1-x}Al_xAs$ semiconductor QWs, within the effective-mass approximation. Non-parabolic and anisotropy effects are taken into account within the Ogg-McCombe effective Hamiltonian[31,32] used to describe the electron states in the semiconductor heterostructure. Both the cyclotron effective mass and $g_\perp$-factor are obtained as functions of the in-plane magnetic field, cyclotron orbit-center position,[33–35] and QW width, and theoretical results compare quite well with available experimental measurements for the $g_\perp$-factor by Hannak *et al.*,[16] Le Jeune *et al.*,[17] and Malinowski *et al.*[18] The work is organized as follows. The theoretical framework is outlined in Sec. II. Results and discussion are performed in Sec. III, and final conclusions are in Sec. IV.

## II. THEORETICAL FRAMEWORK

We consider the problem of a conduction-band electron in a GaAs-$Ga_{1-x}Al_xAs$ QW, grown along the $y$ axis, under an

 

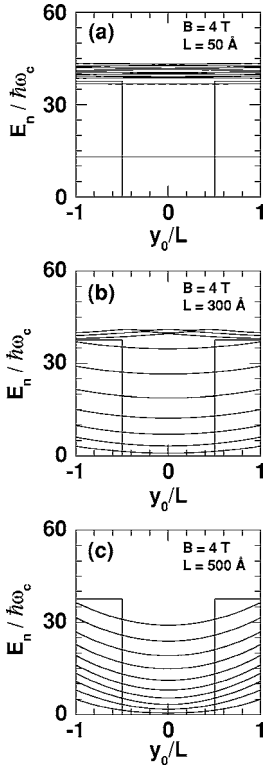


FIG. 1. Orbit-center position dependence of the 10 lowest Landau levels in GaAs-$Ga_{0.65}Al_{0.35}As$ QWs, of width $L$, under a $B=4$ T in-plane magnetic field, for $L=50$ Å (a), $L=300$ Å (b), and $L=500$ Å (c), respectively. Solid and dashed lines correspond to the spin-up ($\uparrow$) and spin-down ($\downarrow$) cases, respectively, although they are essentially undistinguishable for the scale used in the figure. The potential profile is shown schematically.

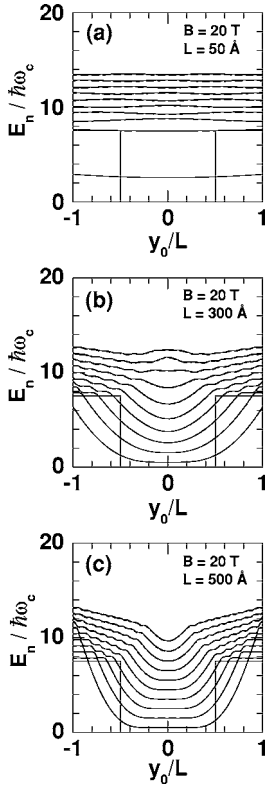


FIG. 2. As in Fig. 1, for $B=20$ T.

in-plane $\mathbf{B}=B\hat{z}$ magnetic field. Here we adopt the effective-mass approximation, and take into account non-parabolicity effects for the conduction electrons, as detailed in previous theoretical work.[31,32,36–39] Present calculations therefore use an Ogg-McCombe effective Hamiltonian[31,32] for the conduction electrons, which is given by

$$\hat{H}=\frac{\hbar^2}{2}\hat{\mathbf{K}}\frac{1}{m(y)}\hat{\mathbf{K}}+\frac{1}{2}g(y)\mu_B\hat{\sigma}_z B+\Gamma\hat{\sigma}\cdot\hat{\tau}+a_1\hat{\mathbf{K}}^4+\frac{a_2}{l_B^4}+a_3[\{\hat{K}_x^2,\hat{K}_y^2\}+\{\hat{K}_x^2,\hat{K}_z^2\}+\{\hat{K}_y^2,\hat{K}_z^2\}]+a_4B\hat{\mathbf{K}}^2\hat{\sigma}_z+a_5\{\hat{\sigma}\cdot\hat{\mathbf{K}},\hat{K}_z B\}+a_6B\hat{\sigma}_z\hat{K}_z^2+V(y), \quad (1)$$

where $\hat{\mathbf{K}}=\hat{\mathbf{k}}+(e/\hbar c)\hat{\mathbf{A}}$, $\hat{\mathbf{k}}=-i\nabla$; $\hat{\mathbf{A}}=(-yB,0,0)$ is the magnetic vector potential, $\hat{\sigma}=(\hat{\sigma}_x,\hat{\sigma}_y,\hat{\sigma}_z)$, where the $\hat{\sigma}_i$ are the Pauli matrices, $\hat{\tau}$ is a vector operator with components given as $\hat{\tau}_x=\hat{K}_y\hat{K}_x\hat{K}_y-\hat{K}_z\hat{K}_x\hat{K}_z$ and corresponding cyclic permutations, $m(y)$ and $g(y)$ are the growth-direction position-dependent (with bulk values of GaAs or $Ga_{1-x}Al_xAs$) conduction-electron effective mass[40] and Landé $g$-factor,[41] respectively, $\mu_B$ is the Bohr magneton, $\Gamma$ is a constant associated with the cubic Dresselhaus spin-orbit term,[42] $l_B=\sqrt{\hbar c/eB}$ is the Landau length, $\{\hat{a},\hat{b}\}=\hat{a}\hat{b}+\hat{b}\hat{a}$ is the anti-commutator between the $\hat{a}$ and $\hat{b}$ operators, and $V(y)$ is the confining potential, taken as 60% of the $Ga_{1-x}Al_xAs$ and GaAs band-gap offset[43–47] $\Delta E_g(\mathrm{eV})=1.247\,x$. Here we note that non-parabolicity effects are taken into account via the coupling between the lowest $\Gamma_{6c}$ conduction band, $\Gamma_{7v}$ and $\Gamma_{8v}$ valence bands, and the $\Gamma_{7c}$ and $\Gamma_{8c}$ $p$-antibonding conduction bands in GaAs. This leads to a $14\times14$ matrix Hamiltonian, which may be folded back into a $2\times2$ conduction-band effective Hamiltonian.[36,37,48–50] One then would expect an adequate theoretical description of the conduction-band Landau levels in zinc-blende-type semiconductors, semiconductor QWs, heterostructures, etc. The second term in the Hamiltonian is the Zeeman contribution, the third one, of third order in $\mathbf{K}$, is the spin-orbit Dresselhaus interaction[42] (due to the fact that GaAs has no inversion symmetry) which, together with the second-order in $\mathbf{K}$ spin-dependent terms (with the factors $a_4, a_5$, and $a_6$), contributes to changes in the effective heterostructure $g$ factor. The term with the factor $a_2$ gives the diamagnetic shift of the Landau electronic levels, whereas terms in $a_1$ and $a_3$ govern the energy dependence of the cyclotron effective mass. In the above Hamiltonian, $a_1, a_2, a_3, a_4, a_5$, and $a_6$ are constants appropriate to bulk GaAs obtained via a fitting with magneto-spectroscopic measurements.[37]

We choose the eigenfunction of (1) as

$$\begin{pmatrix}\varphi(\mathbf{r})\\ \phi(\mathbf{r})\end{pmatrix}=\frac{e^{i(xk_x+zk_z)}}{\sqrt{S}}\begin{pmatrix}\psi_{n,y_0,\uparrow}(y-y_0)\\ \psi_{n,y_0,\downarrow}(y-y_0)\end{pmatrix}, \quad (2)$$

where $n$ is the Landau magnetic-subband index, and the cyclotron orbit-center position $y_0=k_x l_B^2$ is a good quantum num-

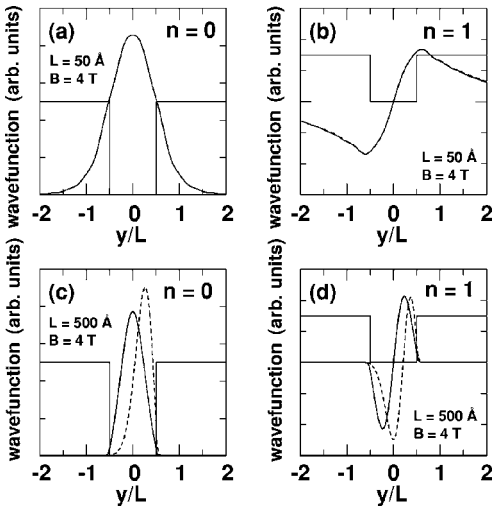


FIG. 3. Electron wave functions for $n=0$ [(a) and (c)] and $n=1$ [(b) and (d)] in GaAs-$Ga_{0.65}Al_{0.35}As$ QWs under a $B=4$ T in-plane magnetic field. Results displayed in (a) and (b), and in (c) and (d) were obtained for $L=50$ Å and $L=500$ Å, respectively. The orbit-center position is at the center (solid curve) and at the right edge (dashed line) of the QW. Results for spin-up and spin-down are undistinguishable in the figure.

ber. In the absence of the confining potential, the eigenvalues of (1) do not depend on the cyclotron orbit-center position $y_0$, and as a consequence, they are infinitely degenerated in $k_x$. The confining potential breaks off this degeneracy, and the eigenvalues of (1) become dispersive. At low temperatures, one may disregard the $k_z$ energy dependence, take $k_z=0$, and by neglecting the off-diagonal terms[51–54] in the Schrödinger equation, the $\uparrow$ spin-up and $\downarrow$ spin-down states are uncoupled. The Schrödinger equation is then given by

$$\begin{pmatrix} \hat{H}_\uparrow & 0 \\ 0 & \hat{H}_\downarrow \end{pmatrix} \begin{pmatrix} \psi_{n,y_0,\uparrow}(y-y_0) \\ \psi_{n,y_0,\downarrow}(y-y_0) \end{pmatrix} = E \begin{pmatrix} \psi_{n,y_0,\uparrow}(y-y_0) \\ \psi_{n,y_0,\downarrow}(y-y_0) \end{pmatrix}, \quad (3)$$

where $\hat{H}_\uparrow$ and $\hat{H}_\downarrow$ are the diagonal components of (1) for $k_z=0$. For a given $m_s$ projection ($\uparrow$ or $\downarrow$), along the magnetic-field direction, of the electron spin we expand the corresponding wave functions in terms of the solutions of the harmonic oscillator problem,

$$\psi_{n,y_0,m_s}(y-y_0) = \sum_m c_{nm}(y_0,m_s)|m,y_0\rangle, \quad (4)$$

with

$$|m,y_0\rangle = \sqrt{\frac{1}{2^m m!\sqrt{\pi} l_B}} e^{-(1/2l_B^2)(y-y_0)^2} H_m\left(\frac{y-y_0}{l_B}\right), \quad (5)$$

where $H_m$ are the Hermite polynomials. The wave functions (4) satisfy the Schrödinger equation

$$\hat{H}_{m_s}\psi_{n,y_0,m_s}(y-y_0) = E_n(y_0,m_s)\psi_{n,y_0,m_s}(y-y_0), \quad (6)$$

and one obtains

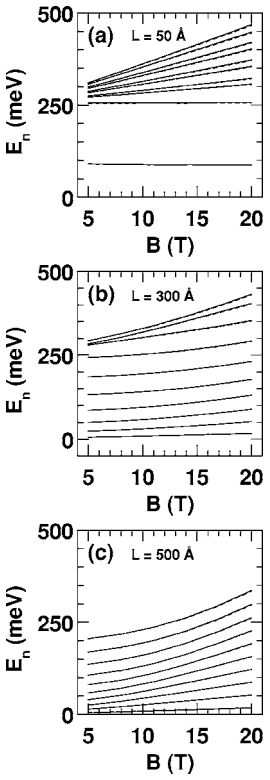


FIG. 4. Dependence of the 10 lowest Landau levels on the in-plane magnetic fields for an orbit-center position at the center of the GaAs-$Ga_{0.65}Al_{0.35}As$ QW. Solid and dashed lines correspond to the spin-up and spin-down cases, respectively; (a), (b), and (c) are for $L=50$ Å, $L=300$ Å, and $L=500$ Å, respectively.

$$\sum_m (H_{m_s}^{(j,m)} - E_n(y_0,m_s)\delta_{j,m})c_{n,m}(y_0,m_s) = 0, \quad (7)$$

leading to an eigenvalue and/or eigenvector problem and the straightforward diagonalization of $\hat{H}_{m_s}$ until convergence of the eigenvalues $E_n(y_0,m_s)$ is achieved. We would like to stress that the terms of order superior than the parabolic ($\hat{K}^2$) in (1) are quite often taken into account via perturbation theory,[48–50,55,56] and in the present work they are exactly considered within the diagonal approach.

## III. RESULTS AND DISCUSSION

As the experimental data from Hannak *et al.*,[16] Le Jeune *et al.*,[17] and Malinowski *et al.*[18] on the electronic Landé $g_\perp$ factor are for GaAs-$Ga_{1-x}Al_xAs$ QWs with Al proportion corresponding to $x=0.35$, results discussed in this section refer to GaAs-$Ga_{0.65}Al_{0.35}As$ QWs under in-plane magnetic fields.

In Fig. 1 we display the 10 lowest Landau levels as functions of the orbit-center position in GaAs-$Ga_{0.65}Al_{0.35}As$ QWs under an in-plane magnetic field of $B=4$ T. The orbit-center position is in units of the well width $L$, and energies in units of the cyclotron energy $\hbar\omega_c=\hbar eB/m_w c$, where $m_w$ is the conduction electron effective mass in the well material, i.e., in GaAs. Figures 1(a)–1(c) correspond to QW widths $L=50$ Å, $L=300$ Å, and $L=500$ Å, respectively, whereas

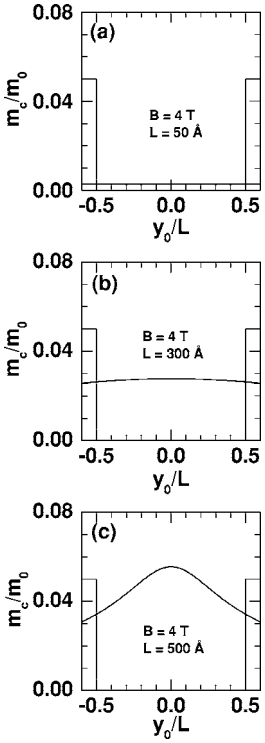


FIG. 5. Orbit-center position dependence of the cyclotron effective mass in GaAs-$Ga_{0.65}Al_{0.35}As$ QWs under a $B=4$ T in-plane magnetic field. The orbit-center position and the cyclotron effective mass are expressed in units of the well width and of the free-electron mass, respectively; (a), (b), and (c) were obtained for $L=50$ Å, $L=300$ Å, and $L=500$ Å, respectively. Solid and dashed lines correspond to the spin-up and spin-down, respectively, although they are undistinguishable in the figure. The potential profile is also shown.

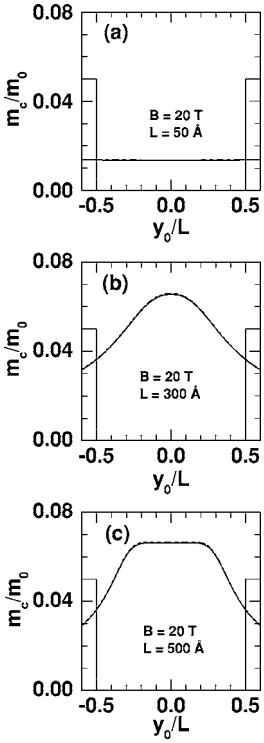


FIG. 6. As in Fig. 5, for $B=20$ T.

solid and dashed lines are associated with the Landau electron subbands with spin projections in the parallel ($\uparrow$) and antiparallel ($\downarrow$) directions of the in-plane applied magnetic field along the $+z$ axis, respectively. Note that the $\uparrow$ and $\downarrow$ electron subbands are essentially undistinguishable for the scale used in Fig. 1. Also, as one may notice from Fig. 1(a), for an $L=50$ Å GaAs-$Ga_{0.65}Al_{0.35}As$ QW, and in the range of $y_0$ orbit center considered, the lowest Landau energy subbands are essentially flat as a function of the orbit-center position. This behavior is to be expected for small values of the applied magnetic field, as the QW width of 50 Å is small compared with the ($B=4$ T) $l_B=128$ Å Landau length. Therefore, in this case ($L \ll l_B$), the effect of the magnetic field is weak and the electronic Landau energy-level structure is essentially dominated by the barrier confining potential. As the GaAs-$Ga_{0.65}Al_{0.35}As$ QW width is increased beyond the $l_B$ Landau length, the orbit-center position dependence of the electron Landau subbands becomes dispersive [cf. Figs. 1(b) and 1(c)], with a minimum at the center of the well, i.e., $y_0=0$. At low temperatures, therefore, electrons would tend to populate energy levels around $y_0=0$. The same calculation was performed for $B=20$ $T$ ($l_B=57$ Å), and shown in Fig. 2. Notice that the orbit-center dependence of the electron Landau levels is more dramatic as compared with results in Fig. 1. The behavior of the Landau levels as functions of the orbit-center position may be understood in terms of the wave function localization: the lowest electron states are essentially localized inside the GaAs-$Ga_{0.65}Al_{0.35}As$ QW due to the barrier or magnetic-field effects on the electron confinement, and the localization region (and the electron energy) is sensitive with respect to the orbit-center position. Notice that when the distance between $y_0$ and $L/2$ is $\lesssim l_B$, the barrier-potential effects are quite appreciable. Figure 3 shows the electron wave function for the $n=0$ [Figs. 3(a) and 3(c)] and for the $n=1$ [Figs. 3(b) and 3(d)] Landau levels in GaAs-$Ga_{0.65}Al_{0.35}As$ QWs of width $L=50$ Å [Figs. 3(a) and 3(b)] and $L=500$ Å [Figs. 3(c) and 3(d)] under an in-plane magnetic field of $B=4$ T. Solid and dashed lines correspond to the orbit-center position at the center and at the right edge of the QW, respectively. Results for $\uparrow$ and $\downarrow$ spin states are essentially the same in the scale used for plotting the wave functions. Note that, for $L=50$ Å QWs [Figs. 3(a) and 3(b)], the wave functions for orbit-center positions at the well-center and well-edge are indistinguishable, as $L \ll l_B$, and the Landau subbands are flat with the barrier-potential effects dominant.

In the present study, we are interested in comparing our calculations with low-temperature experimental measurements,[16–18] in which only the lowest-energy states are occupied. Therefore, one may consider only states with the orbit-center position at the center of the well ($y_0=0$ or $k_x=0$). In Fig. 4 we display, for $y_0=0$, the in-plane magnetic-field dependence of the lowest 10 Landau levels in GaAs-$Ga_{0.65}Al_{0.35}As$ QWs of widths $L=50$ Å, $L=300$ Å, and $L=500$ Å. It is apparent that, as the in-plane magnetic field is increased, the electron wave functions become more localized, and the corresponding energies increase. Also, one notices that the difference between the energies corresponding

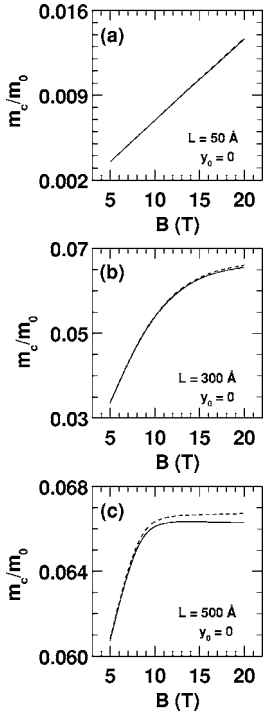


FIG. 7. The cyclotron effective mass as a function of the in-plane magnetic field in GaAs-$Ga_{0.65}Al_{0.35}As$ QWs, of width $L$, for (a) $L$=50 Å, (b) $L$=300 Å, and (c) $L$=500 Å. The orbit-center position was taken at the center of the well. Solid and dashed lines correspond to spin-up and spin-down, respectively.

to the ↑ and ↓ spin states (although quite minor in the scale of Fig. 4) is more noticeable for higher values of the applied magnetic field.

As it is well known, the technique of cyclotron resonance is a powerful tool in the study of the effective mass and transport properties of electrons in semiconductor heterostructures. An in-plane magnetic field may modify the cyclotron effective mass due to the distortion of the Fermi contour by the applied field. In that respect, the inclusion of the band non-parabolicity is crucial in order to obtain a proper quantitative agreement with experimental measurements. For a given projection $m_s$ of the electron spin, the $m_c$ cyclotron effective mass associated with the $n$th and $(n+1)$th Landau magnetic subbands may be defined by

$$E_{n+1}(y_0,m_s) - E_n(y_0,m_s) = \hbar\frac{eB}{m_c c}. \tag{8}$$

The cyclotron effective mass (for $n$=0 in the above equation) is shown in Fig. 5 as a function of the orbit-center position in GaAs-$Ga_{0.65}Al_{0.35}As$ QWs of width $L$=50 Å, $L$ =300 Å, and $L$=500 Å, under an in-plane magnetic field of $B$=4 T. For $L$=50 Å [Fig. 5(a)] the orbit-center position dependence of the cyclotron effective mass is flat, which is due to the fact that the Landau energy levels are essentially independent of the orbit-center position [see Fig. 1(a)]. Moreover, the cyclotron effective mass is 20 times smaller than the bulk GaAs electron effective mass. One may argue that this is due to the large difference, due to the barrier confinement effects, between the energies corresponding to the ground and first-excited Landau levels. For $L \gg l_B$, the cyclotron effective mass increases and tends to the bulk GaAs electron effective mass for the orbit-center position at the center of the well, as expected. This fact is clearly observed in Fig. 6, for $B$=20 T. As the magnetic field increases, the effect of the barrier confining potential becomes less important than the magnetic-field confining effect, the cyclotron effective mass increases, and for very large magnetic fields ($L \gg l_B$), the difference between the $n$=1 and $n$=0 Landau levels is essentially given by $\hbar\omega_c = \hbar eB/m_w c$, and $m_c \to m_w$. Figure 7 displays the magnetic-field dependence of the cyclotron effective mass in GaAs-$Ga_{0.65}Al_{0.35}As$ QWs, for the orbit-center position at the center of the QW, and for well widths of $L$=50 Å, $L$=300 Å, and $L$=500 Å. For large values of the well width and in-plane magnetic fields, i.e., $L \gg l_B$, the electron wave functions are essentially localized inside the GaAs layer, and the cyclotron-effective mass is very close to the GaAs-bulk electron-effective mass [see Fig. 7(c)].

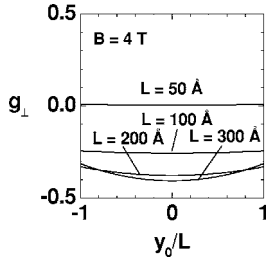


FIG. 8. $g_\perp$ factor as a function of the orbit-center position in GaAs-$Ga_{0.65}Al_{0.35}As$ QWs. Results are shown for various values of the width and for $B$=4 T.

With respect to the $g_\perp$ factor, the expression

$$\Delta E_n = E_n(y_0,\uparrow,B) - E_n(y_0,\downarrow,B) = g_\perp^{(n)}\mu_B B, \tag{9}$$

may be used to define the $g_\perp^{(n)}$ effective Landé factor in the in-plane direction (perpendicular to the $y$-growth axis) associated to the $E_n(y_0,m_s,B)$ Landau levels. In Eq. (9) the explicit dependence of the Landau levels on the applied in-plane magnetic field is displayed. Notice that Eq. (9) is an adequate way of defining the $g_\perp^{(n)}$ effective Landé factor due to the fact that the ↑ and ↓ spin states, in the present calculations, are decoupled. Moreover, it is clear that the effective $g_\perp^{(n)}$ factor will, in principle, depend on the orbit-center position, on the applied magnetic field, and on the QW width. This dependence is illustrated in Figs. 8–10 for the $g_\perp^{(1)}$ factor corresponding to the Landau magnetic levels in GaAs-$Ga_{0.65}Al_{0.35}As$ QWs. The orbit-center position dependence of the $g_\perp$ factor is shown in Fig. 8 for $B$=4 T and for various values of the well width. As the electron-Landau levels are essentially flat for $B$=4 T, $L$=50 Å and $L$=100 Å, for these values of the QW width, the $g_\perp$ factor does not appreciably depend on the orbit-center position. As the QW width increases beyond $l_B$, the orbit-center position dependence of the $g_\perp$ factor becomes appreciable (note that the difference between the Landé factors corresponding to $y_0 = L/2$ and $y_0$ =0 are ~5% for $L$=300 Å). In Fig. 9 we display the

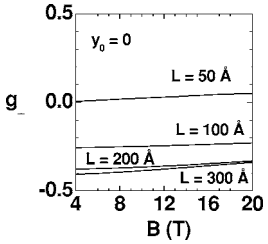


FIG. 9. $g_\perp$ factor as a function of the applied magnetic field in GaAs-$Ga_{0.65}Al_{0.35}As$ QWs. Results are shown for various values of the width and for the orbit-center position at the center of the well.

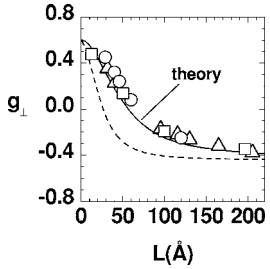


FIG. 10. $g_\perp$ factor as a function of the QW width in GaAs-$Ga_{0.65}Al_{0.35}As$ QWs. Theoretical results (full curve) are shown for $B=4$ T and for the orbit-center position at the center of the well (the dashed curve corresponds to theoretical results obtained by using $a_1=a_2=\cdots=a_6=0$). Squares, circles, and triangles are the experimental data from Hannak *et al.* (Ref. 16), Le Jeune *et al.* (Ref. 17), and Malinowski *et al.* (Ref. 18), respectively.

magnetic-field dependence of the $g_\perp$ factor for various values of the QW width, and for the orbit-center position at the center of each QW. Results were obtained for magnetic fields from 4 T to 20 T. In these range of magnetic-field values, it is apparent that the $g_\perp$ factor weakly depends on the applied in-plane magnetic field. The field dependence on the $g_\perp$ factor is due both by the modification of the energy band structure as well as by the redistribution of the wave function by the magnetic field. Results in Fig. 9 may be understood as follows. In the range of magnetic fields considered, the Landau length varies from $l_B=128$ Å (for $B=4$ T) to $l_B=57$ Å (for $B=20$ T), which implies that, for $L=50$ Å and $L=100$ Å, $l_B > L/2$ and the influence of the barriers on the Landau levels are stronger than that of the magnetic field. The resulting energies of electron Landau states and $g_\perp$ factor are then slowly varying functions of the magnetic field. On the other hand, for $y_0=0$ and $l_B \lesssim L/2$, the influence of the magnetic field is much stronger than that of the barriers, and, therefore, the $g_\perp$ factor weakly depends on the QW widths as shown in Fig. 9 for $L=200$ Å and $L=300$ Å. Finally, we show in Fig. 10 the $g_\perp$ factor as a function of the QW width for $B=4$ T and for the orbit-center position at the center of the well (solid line). The sign of the electron-$g$ factors in the GaAs well and in the $Ga_{0.65}Al_{0.35}As$ barrier are opposite. For the orbit-center position at the center of the QW and for small values of the QW width ($L \ll l_B$), the ground-state electron wave function easily penetrates the $Ga_{0.65}Al_{0.35}As$ barriers, and the $g_\perp$ factor is positive. On the other hand, for large values of the QW widths ($L \gg l_B$), the $g_\perp$ factor is negative due essentially to the localization of the ground-state electron wave function in the well material. Therefore, there must be a well thickness where the $g_\perp$ factor is zero. This is clearly observed in Fig. 10. The experimental results (at $B=4$ T) from Hannak *et al.*[16] (for $B$ in the range from 1 T to 14 T), Le Jeune *et al.*[17] (for $B$ in the range from 1 T to 4 T), and Malinowski *et al.*[18] (for $B=4$ T) are also represented by squares, circles, and triangles, respectively. One may note that the present theoretical calculations (full curve in Fig. 10) are in excellent agreement with the experimental measurements. Also, it is interesting to stress that the effects of the non-parabolic terms are quite important, as one may see from the calculated results obtained by ignoring non-parabolic effects (see dashed curve in Fig. 10), i.e., by setting $a_i=0$, $i=1,2,\ldots,6$.

## IV. CONCLUSIONS

In summary, we have theoretically evaluated the effects of an in-plane magnetic field on the cyclotron effective mass and Landé $g_\perp$ factor in single GaAs-(Ga,Al)As QWs. Present calculations were performed within the effective-mass approximation, and by taking into account the non-parabolic-band effects via the Ogg-McCombe effective Hamiltonian, which was used for the conduction electrons in the GaAs-(Ga,Al)As heterostructure. The characteristic problem of this Hamiltonian, which is usually solved by perturbation theory, in the present work is solved by expanding the corresponding spin-up ($\uparrow$) and spin-down ($\downarrow$) envelope wave functions in terms of the harmonic-oscillator wave functions, considering all of its terms on equal footing. We have obtained both the cyclotron effective mass and the $g_\perp$ factor as a function of the in-plane magnetic field, of the orbit-center position, and of the QW widths. For orbit-center positions at the center of the QW, results for the Landé $g_\perp$ factor were found weakly dependent on the applied magnetic field. Moreover, the QW-width dependence $g_\perp$ factor reveals, as expected, a change in its sign, a fact which may be understood in terms of the electron wave function localization. Present theoretical calculations for the Landé $g_\perp$ factor in single GaAs-(Ga,Al)As quantum wells were found in excellent agreement with the experimental measurements reported by Hannak *et al.*,[16] Le Jeune *et al.*,[17] and Malinowski *et al.*[18]

## ACKNOWLEDGMENTS

The authors would like to thank the Brazilian Agencies CNPq, FAPESP, Rede Nacional de Materiais Nanoestruturados/CNPq, and MCT-Millenium Institute for Quantum Computing/MCT for partial financial support. Two of the authors (M.dD.L. and E.R.G.) wish to thank the warm hospitality of the Institute of Physics, State University of Campinas, Brazil, where part of this work was performed.

[1] M. Bode, M. Getzlaff, and R. Wiesendanger, Phys. Rev. Lett. **81**, 4256 (1998).
[2] S. Heinze, M. Bode, A. Kubetzka, O. Pietzsch, X. Nie, S. Blugel, and R. Wiesendanger, Science **288**, 1805 (2000).
[3] Z. Nussinov, M. F. Crommie, and A. V. Balatsky, Phys. Rev. B **68**, 085402 (2003).
[4] Michael A. Nielsen and Isaac L. Chuang, *Quantum Computation and Quantum Information* (Cambridge University Press, Cambridge, 2000).
[5] G. Salis, Y. K. Kato, K. Ensslin, D. C. Driscol, A. C. Gossard, and D. D. Awschalom, Nature **414**, 619 (2001).
[6] I. Zutic, J. Fabian, and S. Das Sarma, Rev. Mod. Phys. **76**, 323 (2004).
[7] H-A. Engel and D. Loss, Science **309**, 586 (2005).
[8] F. A. P. Osório, M. H. Degani, and O. Hipólito, Phys. Rev. B **38**, 8477 (1988).
[9] R. J. Nicholas, M. A. Hopkins, D. J. Barnes, M. A. Brummell, H. Sigg, D. Heitmann, K. Ensslin, J. J. Harris, C. T. Foxon, and G. Weimann, Phys. Rev. B **39**, 10955 (1989).
[10] S. Huant, A. Mandray, and B. Etienne, Phys. Rev. B **46**, 2613 (1992).
[11] B. E. Cole, J. M. Chamberlain, M. Henini, T. Cheng, W. Batty, A. Wittlin, J. A. A. J. Perenboom, A. Ardavan, A. Polisski, and J. Singleton, Phys. Rev. B **55**, 2503 (1997).
[12] G. R. Johnson, A. Kana-ah, B. C. Cavenett, M. S. Skolnick, and S. J. Baas, Semicond. Sci. Technol. **2**, 182 (1987).
[13] M. Dobers, K. v. Klitzing, and G. Weimann, Phys. Rev. B **38**, 5453 (1988).
[14] M. J. Snelling, G. P. Flinn, A. S. Plaut, R. T. Harley, A. C. Tropper, R. Eccleston, and C. C. Phillips, Phys. Rev. B **44**, 11345 (1991).
[15] A. P. Heberle, W. W. Rühle, and K. Ploog, Phys. Rev. Lett. **72**, 3887 (1994).
[16] R. M. Hannak, M. Oestreich, A. P. Heberle, W. W. Ruhle, and K. Kohler, Solid State Commun. **93**, 313 (1995).
[17] P. Le Jeune, D. Robart, X. Marie, T. Amand, M. Brosseau, J. Barrau, V. Kalevich, and D. Rodichev, Semicond. Sci. Technol. **12**, 380 (1997).
[18] A. Malinowski and R. T. Harley, Phys. Rev. B **62**, 2051 (2000).
[19] V. F. Sapega, T. Ruf, M. Cardona, K. Ploog, E. L. Ivchenko, and D. N. Mirlin, Phys. Rev. B **50**, 2510 (1994).
[20] G. Medeiros-Ribeiro, M. V. B. Pinheiro, V. L. Pimentel, and E. Marega, Appl. Phys. Lett. **80**, 4229 (2002).
[21] S. Lindermann, T. Ihn, T. Heinzel, W. Zwerger, K. Ensslin, K. Maranowski, and A. C. Gossard, Phys. Rev. B **66**, 195314 (2002).
[22] R. Hanson, B. Witkamp, L. M. K. Vandersypen, L. H. Willems van Beveren, J. M. Elzerman, and L. P. Kouwenhoven, Phys. Rev. Lett. **91**, 196802 (2003).
[23] D. K. Maude, M. Potemski, J. C. Portal, M. Henini, L. Eaves, G. Hill, and M. A. Pate, Phys. Rev. Lett. **77**, 4604 (1996).
[24] Y. K. Kato, R. C. Myers, D. C. Driscol, A. C. Gossard, J. Levy, and D. D. Awschalom, Science **299**, 1201 (2003).
[25] Y. K. Kato, R. C. Myers, A. C. Gossard, and D. D. Awschalom, Science **306**, 1910 (2004).
[26] A. S. Bracker, E. A. Stinaff, D. Gammon, M. E. Ware, J. G. Tischler, A. Shabaev, Al. L. Efros, D. Park, D. Gershoni, V. L. Korenev, and I. A. Merkulov, Phys. Rev. Lett. **94**, 047402 (2005).
[27] E. I. Rashba and A. L. Efros, Phys. Rev. Lett. **91**, 126405 (2003).
[28] R. de Sousa and S. Das Sarma, Phys. Rev. B **68**, 155330 (2003).
[29] S. J. Prado, C. Trallero-Giner, A. M. Alcalde, V. Lopez-Richard, and G. E. Marques, Phys. Rev. B **69**, 201310(R) (2004).
[30] C. F. Destefani and S. E. Ulloa, Phys. Rev. B **71**, 161303(R) (2005).
[31] N. R. Ogg, Proc. Phys. Soc. London **89**, 431 (1966).
[32] B. O. McCombe, Phys. Rev. **181**, 1206 (1969).
[33] J. C. Maan, in *Festkörperprobleme*, edited by P. Grosse, Advances in Solid State Physics, Vol. 27 (Vieweg, Braunschweig, 1987), p. 137.
[34] J. C. Maan, Surf. Sci. **196**, 518 (1988).
[35] G. Platero and M. Altarelli, Phys. Rev. B **39**, 3758 (1989).
[36] M. Braun and U. Rössler, J. Phys. C **18**, 3365 (1985).
[37] V. G. Golubev, V. I. Ivanov-Omskii, I. G. Minervin, A. V. Osutin, and D. G. Polyakov, Sov. Phys. JETP **61**, 1214 (1985).
[38] J. Sabín del Valle, J. López-Gondar, and M. de Dios-Leyva, Phys. Status Solidi B **151**, 127 (1989).
[39] A. Bruno-Alfonso, L. Diago-Cisneros, and M. de Dios-Leyva, J. Appl. Phys. **77**, 2837 (1995).
[40] E. H. Li, Physica E (Amsterdam) **5**, 215 (2000).
[41] C. Hermann and C. Weisbuch, Phys. Rev. B **15**, 823 (1977).
[42] G. Dresselhaus, Phys. Rev. **100**, 580 (1955).
[43] R. C. Casey, Jr., J. Appl. Phys. **49**, 3684 (1978).
[44] Depending on the Al content of $Ga_{1-x}Al_xAs$, its band gap may be blueshifted as much as 445 meV from the GaAs bulk value (Ref. 45). The band-gap discontinuity in the GaAs-$Ga_{1-x}Al_xAs$ heterostructure was considered, for about a full decade, and according to Dingle (Ref. 45), as distributed 85% on the valence band and 15% on the conduction band. However, Miller *et al.* (Ref. 46) proposed a 57%–43% split in order to better explain their optical data, whereas Wang *et al.* (Ref. 47) found that a 62%–38% split would be more appropriate to explain charge-transfer measurements in *p*-type modulation-doped GaAs-$Ga_{1-x}Al_xAs$ heterostructures and, since then, these values were widely accepted by specialists in the field. Here, therefore, we adopt a 60%–40% choice for the split.
[45] R. Dingle, in *Festkörperprobleme XV*, edited by H. J. Queisser (Pergamon, Braunschweig, 1975), p. 21.
[46] R. C. Miller, D. A. Kleinman, and A. C. Gossard, Phys. Rev. B **29**, 7085 (1984).
[47] W. Wang, E. E. Mendez, and F. Stern, Appl. Phys. Lett. **45**, 639 (1984).
[48] G. Lommer, F. Malcher, and U. Rössler, Phys. Rev. B **32**, 6965 (1985).
[49] F. Malcher, G. Lommer, and U. Rössler, Superlattices Microstruct. **2**, 267 (1986).
[50] G. Lommer, F. Malcher, and U. Rössler, Superlattices Microstruct. **2**, 273 (1986).
[51] Here we note that the diagonal and $k_z=0$ approximations result in disregarding effects of the $\Gamma\hat{\sigma}\cdot\hat{\tau}$ Dresselhaus (Ref. 42) contribution, which is nonzero due to the presence of terms in $\hat{\sigma}_x$ and $\hat{\sigma}_y$. For values (Refs. 28, 37, 38, 52, and 53) of $\Gamma\approx$ 20–30 eV Å$^3$, the contribution to the energy levels of the Dresselhaus term may be shown to be $\lesssim$0.1 meV (see discussion by Golubev *et al.* (Ref. 37) and Sabin *et al.* (Ref. 38)]. It is important to notice, however, that one should not underestimate the importance of the Dresselhaus contribution in other phenomena as, for instance, the D'yakonov-Perel' mechanism (Ref. 54) of spin relaxation as thoroughly discussed in a recent review by Zutic *et al.* (Ref. 6).

[52] J. Kainz, U. Rössler, and R. Winkler, Phys. Rev. B **68**, 075322 (2003).
[53] J. Könemann, R. J. Haug, D. K. Maude, V. I. Falko, and B. L. Altshuler, Phys. Rev. Lett. **94**, 226404 (2005).
[54] M. I. D'yakonov and V. I. Perel', Sov. Phys. Solid State **13**, 3023 (1971).
[55] N. Kim, G. C. La Rocca, and S. Rodriguez, Phys. Rev. B **40**, 3001 (1989).
[56] B. Das, S. Datta, and R. Reifenberger, Phys. Rev. B **41**, 8278 (1990).